J. Fluid Mech. (1982), *vol.* 119, *pp.* 423–441
Printed in Great Britain

Simplified theory of the near-wall turbulent layer of Newtonian and drag-reducing fluids

By M. A. GOLDSHTIK, V. V. ZAMETALIN AND V. N. SHTERN

Institute of Thermophysics, Siberian Branch of the U.S.S.R. Academy of Sciences, Novosibirsk-90, 630090, U.S.S.R.

(Received 28 July 1981)

We propose a simplified theory of a viscous layer in near-wall turbulent flow that determines the mean-velocity profile and integral characteristics of velocity fluctuations. The theory is based on the concepts resulting from the experimental data implying a relatively simple almost-ordered structure of fluctuations in close proximity to the wall. On the basis of data on the greatest contribution to transfer processes made by the part of the spectrum associated with the main size of the observed structures, the turbulent fluctuations are simulated by a three-dimensional running wave whose parameters are found from the problem solution. Mathematically the problem reduces to the solution of linearized Navier–Stokes equations. The no-slip condition is satisfied on the wall, whereas on the outer boundary of a viscous layer the conditions of smooth conjunction with the asymptotic shape of velocity and fluctuation-energy profiles resulting from the dimensional analysis are satisfied. The formulation of the problem is completed by the requirement of maximum curvature of the mean-velocity profile on the outer boundary applied from stability considerations.

The solution of the problem does not require any quantitative empirical data, although the conditions of conjunction were formulated according to the well-known concepts obtained experimentally. As a result, the near-wall law for the averaged velocity has been calculated theoretically and is in good agreement with experiment, and the characteristic scales for fluctuations have also been determined. The developed theory is applied to turbulent-flow calculations in Maxwell and Oldroyd media. The elastic properties of fluids are shown to lead to near-wall region reconstruction and its associated drag reduction, as is the case in turbulent flows of dilute polymer solutions. This theory accounts for several features typical of the Toms effect, such as the threshold character of the effect and the decrease in the normal fluctuating velocity. The analysis of the near-wall Oldroyd fluid flow permits us to elucidate several new aspects of the drag-reduction effect. It has been established that the Toms effect does not always result in thickening of the viscous sublayer; on the contrary, the most intense drag reduction takes place without thickening in the viscous sublayer.

1. Introduction

A viscous sublayer plays an important role in transfer processes occurring in turbulent near-wall flow. Maximum values are attained here for the gradients of average velocity, temperature and concentration, for the relative fluctuation ampli-

tudes, and even for the absolute fluctuation energy near the external boundary. On the other hand, the proximity of a wall where the no-slip conditions should be met exerts an ordering effect on the fluctuational motion, leading to the appearance of 'coherent structures' near the wall in the form of streamwise stretched vortex roll-ups. Townsend (1956) was apparently the first to emphasize the role of 'large structures' for the construction of simple models and their main contribution to a turbulent transfer. Detailed experimental visual and electrochemical studies were initiated by Kline *et al.* (1967), Mitchell & Hanratty (1966), Corino & Brodkey (1969) (see also the review of Davies & Yule 1975). The effect of these structures on the statistical characteristics was studied by Repik, Sosedko & Tropinina (1975) and Khabakhpasheva *et al.* (1975).

Certainly the vortex roll-ups observed in a viscous sublayer are not stationary structures, but are akin to flapping flags. Nevertheless, they have definite dimensions reproduced experimentally with a slight scatter. In universal scales (constructed according to the kinematic viscosity ν and velocity $v_* = (\tau_w/\rho)^{\frac{1}{2}}$, where τ_w is the wall shear stress and ρ is the density), the characteristic length of a roll-up is $\sim 10^3$ and the frequency $\sim 0{\cdot}1$. Measurements of two-dimensional fluctuation spectra performed by Morrison, Bullock & Kronauer (1971) indicate that the velocity of disturbance convection does not depend on the distance from the wall, i.e. the motion resembles a running wave.

If the aim is not the detailed analysis of the fluctuation motion but the theoretical calculation of the averaged velocity field, then, bearing in mind that the main contribution to the transfer processes is made by the large-scale part of the spectrum, the fluctuations can be represented schematically as a running three-dimensional wave. Hence the problem of the developed theory is, using this elementary model, to obtain the near-wall law of velocity variations and to determine the wavenumber and the frequency of fluctuations.

A theoretical analysis of the motion in a viscous sublayer was carried out in several studies, beginning with the works of Einstein & Li (1956) and Sternberg (1962) performed in terms of the Stokes equations. Convection terms were taken into account by Schubert & Corcos (1967). Specific features of the turbulent flow in a viscous sublayer were studied by Kader (1970) and Geshev (1974).

Vortex roll-ups in terms of the complete Navier–Stokes equations were calculated by Sadovskii, Sinitzyna & Taganov (1975) and Hatziavramidis & Hanratty (1979). We will not go into details of these studies, but will note only that they all dealt with the empirical numerical data, being the integral part of the models considered. In the present paper we omit any explicit empirical numerical data.

In terms of the formulated theoretical approach, it appeared possible to describe properly the average velocity distribution and some characteristics of the fluctuational motion. To check the applicability of the model in a wider range, it was applied to a theoretical analysis of the drag reduction in a turbulent flow of polymer solutions – the Toms effect (Toms 1948). Here the non-Newtonian character of the medium was taken into account using the Maxwell and Oldroyd rheological models. In terms of the viscoelastic fluid model, the developed theory permits us to describe properly the main features of the drag reduction.

In §2 the problem is formulated for Newtonian liquids. Section 3 represents algorithms for a numerical solution of the formulated problem. In §4 theoretical results

are discussed and compared with experiments on the near-wall flow of the Newtonian fluid. In §5 on the basis of the formulated model theory the near-wall turbulent viscoelastic fluid flow is analysed, and a comparison between theory and experiment on drag reduction in dilute polymer solutions is given. Section 6 extends the analysis for the case of the Oldroyd viscoelastic fluid having stress relaxation and retardation times.

2. Model formulation

A turbulent plane-parallel, on the average, flow near a smooth wall is considered. It is convenient to write down the Navier–Stokes equations separating the averaged and fluctuating velocity components

$$\left.\begin{aligned}
&\frac{\partial v_x}{\partial t}+U\frac{\partial v_x}{\partial x}+v_y U'+\frac{1}{\rho}\frac{\partial p}{\partial x}-\nu\Delta v_x=\frac{\partial}{\partial x_j}\overline{(v_x v_j-v_x v_j)},\\
&\frac{\partial v_y}{\partial t}+U\frac{\partial v_y}{\partial x}+\frac{1}{\rho}\frac{\partial p}{\partial y}-\nu\Delta v_y=\frac{\partial}{\partial x_j}\overline{(v_y v_j-v_y v_j)},\\
&\frac{\partial v_z}{\partial t}+U\frac{\partial v_z}{\partial x}+\frac{1}{\rho}\frac{\partial p}{\partial z}-\nu\Delta v_z=\frac{\partial}{\partial x_j}\overline{(v_z v_j-v_z v_j)},\\
&\frac{\partial v_x}{\partial x}+\frac{\partial v_y}{\partial y}+\frac{\partial v_z}{\partial z}=0,\\
&\nu U'=v_*^2+\overline{v_x v_y};\quad \overline{v_y v_z}=\overline{v_x v_z}=0.
\end{aligned}\right\} \tag{2.1}$$

x- and y-axes were chosen respectively in the streamwise direction and normal to the wall; a bar denotes averaging with respect to the uniform variables x, z and t; a prime denotes differentiation with regard to y.

(*a*) The first simplifying assumption is that in the first three equations of (2.1) the nonlinear-fluctuation terms are removed, the mean-velocity profile is taken as linear $U = U'_{\mathrm{w}} y$ ($U'_{\mathrm{w}} = v_*^2/\nu$) and the solution is found in the form

$$\left.\begin{aligned}
&v_x=\mathscr{R}[u(y)T],\quad v_y=\mathscr{R}[v(y)T],\\
&v_z=\mathscr{R}[w(y)T],\quad p=\mathscr{R}[p(y)T],\\
&T=2^{\frac{1}{2}}\exp\left[i(\alpha x+\beta z)-i\alpha ct\right].
\end{aligned}\right\} \tag{2.2}$$

This assumption is based (i) on the fact that, owing to the no-slip condition, in close proximity to the wall the velocities are small, and (ii) on the conception that the decisive contribution to the transfer process is from the momentum of the fundamental. Certainly, with increasing distance from the wall the neglect of nonlinear terms becomes less and less justifiable and can lead to significant errors. But, we believe, this disadvantage can be removed by taking the appropriate conditions on the outer boundary of the viscous layer to have a nonlinear character. A fluctuation regime is approximated by the sum of two oblique waves (2.2) with opposite sign of β. In this case the last two equations of (2.1) are satisfied automatically.

(*b*) The second reasonable aspect in the model problem is the formulation of the conjunction conditions on the outer boundary of a viscous region which is *a priori* considered to be unknown and is found from the solution. For this purpose let us consider the asymptotic behaviour of the profile of the mean velocity U and of the

fluctuational motion energy $E = \overline{v_x^2 + v_y^2 + v_z^2} = |u| + |v| + |w|$ far from the wall (at $y \to \infty$). Since the effect of viscosity can be neglected, for reasons of dimensionality it follows that $U' = v_*/\kappa y$, where κ is a dimensionless constant. After integration we obtain the known logarithmic distribution

$$U = \frac{v_*}{\kappa} \ln y + B. \tag{2.3}$$

By using the Reynolds equation (the fifth in (2.1)), we obtain the expression for turbulent stresses $-\overline{v_x v_y} = v_*^2 [1 - 1/\kappa y^+]$, where $y^+ = y v_*/\nu$. Naturally, the asymptotic expression for the energy will be the same:

$$E = E_1 v_*^2 \left(1 + \frac{1}{\kappa_1 y^+}\right), \tag{2.4}$$

where E_1 and κ_1 are unknown dimensionless constants. Upon excluding the constants, we obtain a differential form of the asymptotic laws:

$$(yU')' = 0, \quad (yE)'' = 0. \tag{2.5}$$

After substituting (2.2) into (2.1) and eliminating the pressure, we get a system of ordinary differential equations for the amplitudes:

$$v'' - k^2 v = \theta, \quad k^2 = \alpha^2 + \beta^2, \quad \nu\theta'' - [\nu k^2 + i\alpha(v_* y^+ - c)]\theta = 0, \tag{2.6}$$

$$\nu w'' - [\nu k^2 + i\alpha(v_* y^+ - c)] w = \frac{i\beta}{k^2} \{\nu\theta' - i\alpha[(v_* y^+ - c) v' - v U'_{\mathrm{w}}]\}.$$

On the wall the no-slip conditions are met:

$$v(0) = v'(0) = w(0) = 0. \tag{2.7}$$

Far from the wall the conditions without any viscosity effect are set, resulting from (2.6) provided that $\nu = 0$:

$$v'' - k^2 v = 0, \quad w = \frac{i\beta}{k^2} \left[\frac{U'_{\mathrm{w}} v}{v_* y^+ - c} - v'\right]. \tag{2.8}$$

Generally speaking, the conditions (2.5) and (2.8) should be satisfied asymptotically as $y^+ \to \infty$, but here, in a similar manner to the methods of boundary-layer theory, they will be displaced a finite distance from the wall $y^+ = R$, where R can be treated as Reynolds number constructed according to the thickness of the viscous region and the shear velocity v_*.

Now it will be convenient to write down the above equations in dimensionless form, retaining the same designations:

$$\left.\begin{aligned} v'' - k^2 v = \theta, \quad \theta'' - [k^2 + i\alpha(y^+ - c)]\theta = 0, \\ w'' - [k^2 + i\alpha(y^+ - c)] w = \frac{i\beta}{k^2} \{\theta' - i\alpha[(y^+ - c) v' - v]\}, \\ v = v' = w = 0, \quad \theta = 0; \quad w = \frac{i\beta}{k^2} \left[\frac{v}{y^+ - c} - v'\right] \quad \text{at} \quad y^+ = R, \end{aligned}\right\} \tag{2.9}$$

$$(y^+ U')' = 0, \quad (y^+ E)'' = 0 \quad \text{at} \quad y^+ = R, \tag{2.10}$$

where

$$U' = 1 + u_{\mathrm{r}} v_{\mathrm{r}} + u_{\mathrm{i}} v_{\mathrm{i}}, \quad u = i(v' + \beta w)/\alpha \tag{2.11}$$

(indices r and i denote real and imaginary parts of the complex amplitudes).

Equations (2.9) include a system of sixth-order linear equations and five boundary conditions. For given values of α, β, c and R a solution can be found accurate to a constant complex factor, whose argument can be left arbitrary, since it does not influence the calculation of mean characteristics. The factor module is determined from the first condition (2.10) which is of inhomogeneous character owing to (2.11). The second condition (2.10) can be used to determine R. The determination of the parameters α, β and c requires three additional conditions.

(*c*) Formulation of these conditions is the third model assumption which is based on the reasons of stability. Goldshtik (1968) suggested a hypothesis implying that the averaged turbulent motion is maximally stable to the external disturbances. On the other hand, it is known that the presence of inflection points in the velocity profile (see e.g. Goldshtik & Shtern 1977) can cause instabilities. The most sensitive in this respect is the point of conjunction of viscous and external regions. Therefore, let the conditions of conjunction along the mean-velocity profile at $y^+ = R$ be set so that the derivatives up to the fourth can be continuous:

$$(y^+U')'' = 0, \quad (y^+U')''' = 0. \tag{2.12}$$

It will permit us to determine two more parameters, namely α and c. Finally, let us demand that the velocity-profile curvature be maximum:

$$f(\beta) \equiv |U(R)|, \quad \frac{df}{d\beta} = 0. \tag{2.13}$$

Now the totality of (2.9)–(2.13) will be a closed problem whose solution should determine all entering functions and parameters.

Despite the above arguments, it should be said that the assumptions (*a*)–(*c*) do not follow unambiguously from the general reasonings, and contain arbitrary elements. The choice of just these conditions of conjunction is based on the agreement with experiment. Hence the formulation of the problem can be considered to a certain extent as empirical. Nevertheless, its advantage over the previous approaches is that it does not apply any *a priori* empirical information of a quantitative character.

3. Algorithm of solution

The problem (2.9)–(2.13) was solved numerically, the sequence of operations corresponding to the main steps of the formulation.

At constant values of the parameters α, β and c, (2.9) are first integrated. The solution of the second equation of (2.9) can be represented analytically through the Airy function $\theta = D\,\mathrm{Ai}\,(\alpha^{-\frac{2}{3}}[k^2 + i\alpha(y^+ - c)])$, which at large y^+ decreases according to the law $\propto \exp[-(2\alpha)^{\frac{1}{2}}/3(1+i)\,(y^+ - c)^{\frac{3}{2}}]$. Practically, the same solution can be obtained by the numerical integration of the Cauchy problem with the initial data $\theta(R) = 0$, $\theta'(R) = D_1$. The latter condition is the intermediate normalization, and the final value of D (or D_1) is calculated in what follows. Then a Cauchy problem is integrated for the first equation of (2.9) with the initial conditions $v(0) = v'(0) = 0$ using the Runge–Kutta method with a constant step $h = 0{\cdot}5$. Then a boundary-value problem is solved for the function w (2.9) using a difference factorization method, and from (2.11) the function u is determined. Hereby, the function $E(y^+)$ is found,

aside from an unknown factor. $E(y^+)$ increases from zero at $y^+ = 0$, attains a maximum and then begins to decrease. The value of R is determined as the y^+ value at which, for the first time after the maximum E, the condition $(y^+E)'' = 0$ is satisfied. Now the factor D can be calculated from the condition:

$$[y^+(1+u_r v_r + u_i v_i)]' = 0 \quad \text{at} \quad y^+ = R.$$

After multiple repetition of the above procedure for various values of α and c, we choose them using a Newton method, so that the conditions (2.12) be satisfied. Finally, the most external procedure is the search for the β value at which (2.13) is fulfilled. The mean-velocity profile $U(y^+)$ is determined by integration of the first equation (2.11) with the initial condition $U(0) = 0$.

4. Calculation results

The parameters used to solve the problem are

$$\alpha = 0{\cdot}00212, \quad \beta = 0{\cdot}000136, \quad c = 35{\cdot}8, \quad R = 31{\cdot}9, \quad \omega = \alpha c = 0{\cdot}076. \tag{2.14}$$

Constants in the asymptotic equations (2.3) and (2.4) are found from the obtained solutions using the formulas

$$\left.\begin{aligned} \kappa &= \frac{1}{RU'(R)}, \quad B = U(R) - \frac{1}{\kappa}\ln R, \\ \kappa_1 &= -\frac{E(R)+RE'(R)}{R^2E'(R)}, \quad E_1 = \frac{RE(R)}{R+1/\kappa_1}. \end{aligned}\right\} \tag{2.15}$$

Their calculated values are

$$\kappa = 0{\cdot}405, \quad B = 5{\cdot}6, \quad \kappa_1 = 0{\cdot}23, \quad E_1 = 88. \tag{2.16}$$

The first three values are in good agreement with the experimental results of Laufer (1954) and Lawn (1971), and the fourth is significantly higher than the experimental value.

A comparison of the theoretical 'wall law' for the mean-velocity profile with the experimental data is given in figure 1. The solid curve 1 accounts for the theory. The conjunction point is marked by a cross. The dashed line 2 illustrates an analytical continuation of the velocity profile beyond the conjunction point. The curve 3 represents the linear law $U = y^+$, and the straight line 4 is the logarithmic velocity distribution with the calculated constants κ and B. The shaded region shows the scattering of Laufer and Lawn's experimental data. The points are the experimental data of Khabakhpasheva *et al.* (1975) for velocity measurements in the viscous layer.

The agreement between theory and experiment regarding the velocity profile is good, whereas with respect to the velocity fluctuations it is only of a qualitative character, which is confirmed by figure 2. Solid curves account for the theoretical threefold reduced values $|u|$, $|v|$, $|w|$, dashed lines correspond to the Laufer's data and points ($1'-|u|$, $2'-|v|$, $3'-|w|$) were taken from the experimental data of Khabakhpasheva *et al.* This quantitative discrepancy is quite clear, and is associated with a rough schematic representation of fluctuational motion. Note, however, that the position of the $E(y^+)$ maximum at $y^+ = 14$, agrees fairly well with experiment.

According to the calculation, the amplitude of pressure fluctuations is practically constant throughout the viscous layer, which is in agreement with Corcos' theoretical and experimental analysis.

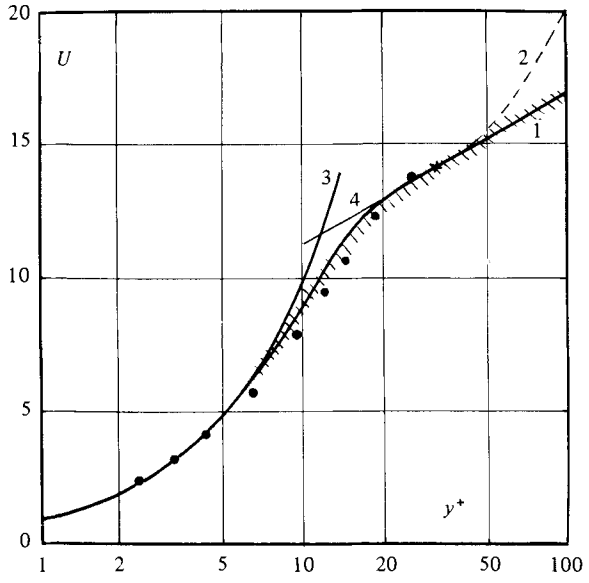

FIGURE 1. Mean-velocity profile near wall: 1, calculation; ×, conjunction point; 2, analytical continuation of the calculated profile; 3, linear law; 4, logarithmic law; shaded part shows experimental data of Laufer (1954) and Lawn (1971); ●, data of Khabakhpasheva *et al.* (1975).

The theoretical fluctuation frequency ω and the longitudinal scale π/α coincide in order of magnitude with experiment. At the same time, visual observations indicate that the width of vortices are an order of magnitude smaller than their length, and the calculated values are in the reverse ratio $\alpha/\beta = 16$. This, however, can be explained. The spectral analysis performed by Corcos, indicates that the disturbances with $\alpha \gg \beta$ and $\alpha \ll \beta$ are predominant; hence the spectrum is concentrated near the axes. A numerical calculation shows that the disturbances with $\alpha \gg \beta$ make a significantly greater contribution to the Reynolds stresses, thus playing the main role in the formation of the mean-velocity profile. But in visual observations the disturbances from the other spectral region with $\alpha \ll \beta$ are more distinct.

Thus, in terms of the above model it is possible to calculate the theoretical distribution of the mean velocity and intensities of fluctuations in the near-wall turbulent flow. Here the velocity profile in a viscous region and the constants for its logarithmic region are calculated. The results are in good agreement with experiment.

What is the field of applicability of the suggested model? Can it be applied to calculate other more-complicated problems concerning near-wall flows? To a certain extent the answer can be the theory of a turbulent near-wall flow of viscoelastic fluid described below, being of interest in relation with the problem of drag reduction in dilute polymer solutions.

5. Drag reduction in Maxwell fluid

At present much attention has been given to the problem of drag reduction in a turbulent flow of fluids containing small polymer additives. Since the drag is significantly reduced at small concentrations of additives when the viscosities of solution and water are practically the same, the determination of the non-Newtonian properties

of dilute solutions responsible for the drag reduction in turbulent flows is a very complicated problem. One of the earliest approaches to the Toms-effect interpretation is the hypothesis of the decisive role of elastic properties of polymer solutions, first suggested, apparently, by Metzner & Park (1964). But at present there is no single point of view on the insight into the mechanism of the drag reduction. Various approaches are based on different rheological models of the tested solutions. But it is very difficult to prove empirically the adequacy of any of these models.

The available semi-empirical models are not suitable for the choice of a rheological model as well, since the dependence of the empirical constants on the rheological properties is unknown, and can be different for different media. Therefore the model theory described in previous sections is advantageous, since it does not involve any empirically determined constants. In this connection, the effect of different rheological properties of fluids on the near-wall turbulent flow will be studied on the basis of the developed sinusoidal theory.

For a previous qualitative analysis we will apply a model of the Maxwell viscoelastic fluid generalized by Oldroyd (1950) for the case of arbitrary deformation. In Cartesian co-ordinates it can be written as

$$\lambda\left(\frac{\partial\Sigma_{ij}}{\partial t}+V_\alpha\frac{\partial\Sigma_{ij}}{\partial x_\alpha}-\frac{\partial V_i}{\partial x_\alpha}\Sigma_{\alpha j}-\frac{\partial V_j}{\partial x_\alpha}\Sigma_{i\alpha}\right)+\Sigma_{ij}=\nu\left(\frac{\partial V_i}{\partial x_j}+\frac{\partial V_j}{\partial x_i}\right), \tag{5.1}$$

where Σ_{ij} is the deviatoric stress tensor, $V_\alpha=\{V_x, V_y, V_z\}$ is the instantaneous velocity vector, and λ is the time of stress relaxation. The system (5.1) in combination with the momentum and continuity equations

$$\frac{\partial V_i}{\partial t}+V_\alpha\frac{\partial V_i}{\partial x_\alpha}=-\frac{\partial P}{\partial x_i}+\frac{\partial\Sigma_{i\alpha}}{\partial x_\alpha},\quad \frac{\partial V_\alpha}{\partial x_\alpha}=0$$

forms a closed system.

Let us consider a problem on the turbulent flow of viscoelastic fluid along an infinite flat plate for which the no-slip conditions and the mean shear stress are set. At infinity it is demanded that the effects of viscosity and elasticity on mean and large-scale characteristics will be absent. It means that we will consider the Prandtl problem for a Maxwell fluid. Given values are shear velocity v_*, viscosity ν, and relaxation time λ. They can be used to constitute two scales of length, i.e. viscous ν/v_* and elastic $v_*\lambda$; hence in terms of the dimensional theory the mean velocity gradient is

$$\frac{dU}{dy}=\frac{v_*}{\kappa y}f\left(\frac{v_* y}{\nu},\frac{y}{v_*\lambda}\right).$$

This representation is typical of the multiple-scale method. If the distance y from the wall is much greater than both viscous and elastic scales, the velocity gradient will be independent of these scales (owing to the arbitrariness of κ, it can be assumed that $f(\infty,\infty)=1$), which leads to the logarithmic velocity distribution.

Now let us consider the behaviour of f at small values of the arguments. After expansion into the Taylor series

$$f=f_0+\frac{v_* y}{\nu}f_{11}+\frac{y}{v_*\lambda}f_{12}+\dots,$$

and satisfaction of the condition $dU/dy=v_*^2/\nu$ at $y=0$, we obtain $f_0=f_{12}=0$, $f_{11}=\kappa$. Whence it follows that, when only the second argument tends to zero, f does not reduce to zero but has a finite limit depending on the first argument.

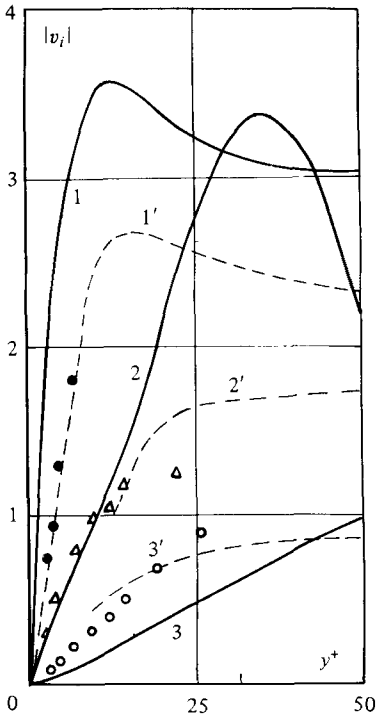

FIGURE 2. Intensities of velocity fluctuations: 1, $|u|$; 2, $|v|$; 3, $|w|$. ——, calculation (threefold reduced); — — — — —, data of Laufer (1954); ●, △, ○, data of Khabakhpasheva *et al.* (1975).

If the elastic scale is much greater than the viscous there exists a range of y values when the first argument can be considered to be infinite and the second to be equal to zero. It means that in this range the velocity also follows the logarithmic law, but generally speaking with other values of the constants. Theoretical conceptions in favour of the existence of an intermediate logarithmic region in the turbulent flow of polymer solutions were given by Gorodtzov & Belokon (1973).

Similar conceptions can also be given for the energy distribution of turbulent fluctuations. The existence of an intermediate asymptotic region permits us to apply the conjunction conditions described in §2 and to close the viscous-layer problem for a non-Newtonian fluid as well.

As above, let us represent the fluid motion as a sum of the fluctuational $\{v_\alpha, \sigma_{ij}, p\}$ and averaged $\{\overline{V}_\alpha, \overline{\sigma}_{ij}, \overline{p}\}$ flows. Taking into account that among the components of $\overline{V}_\alpha$ only the longitudinal velocity $\overline{V}_x = U(y)$ is not equal to zero, the generalized Reynolds equations for Maxwell fluid will be written in the dimensionless form

$$\left.\begin{aligned} \frac{dU}{dy^+}(1+A\overline{\sigma}_{22}) &= 1+\overline{v_x v_y}+A\left[\overline{v_y\left(\frac{\partial\sigma_{11}}{\partial x^+}+\frac{\partial\sigma_{12}}{\partial y^+}+\frac{\partial\sigma_{13}}{\partial z^+}\right)}\right. \\ &\left.+\overline{v_x\left(\frac{\partial\sigma_{21}}{\partial x^+}+\frac{\partial\sigma_{22}}{\partial y^+}+\frac{\partial\sigma_{23}}{\partial z^+}\right)}-\frac{\partial\overline{\sigma_{22}v_x}}{\partial y^+}\right], \\ \overline{\sigma_{22}} &= A\left[\frac{\partial\overline{\sigma_{22}v_y}}{\partial y^+}-2\overline{v_y\left(\frac{\partial\sigma_{21}}{\partial x^+}+\frac{\partial\sigma_{22}}{\partial y^+}+\frac{\partial\sigma_{23}}{\partial z^+}\right)}\right]. \end{aligned}\right\} \tag{5.2}$$

Here $A = \lambda v_x^2/\nu$ is the dimensionless time of relaxation.

After the removal of the terms that are quadratic with respect to fluctuations, the system of equations for a fluctuational motion will take the form

$$\left.\begin{aligned} A\left(\frac{\partial\sigma_{ij}}{\partial t^+}+\overline{V}_\alpha\frac{\partial\sigma_{ij}}{\partial x_\alpha^+}+v_\alpha\frac{\partial\overline{\sigma}_{ij}}{\partial x_\alpha^+}-\frac{\partial v_i}{\partial x_\alpha^+}\overline{\sigma}_{\alpha j}-\frac{\partial\overline{V}_i}{\partial x_\alpha^+}\sigma_{\alpha j}-\frac{\partial v_j}{\partial x_\alpha^+}\overline{\sigma}_{i\alpha}-\frac{\partial\overline{V}_j}{\partial x_\alpha^+}\sigma_{i\alpha}\right)+\sigma_{ij}\\ =\frac{\partial v_i}{\partial x_j^+}+\frac{\partial v_j}{\partial x_i^+},\\ \frac{\partial v_i}{\partial t^+}+\overline{V}_\alpha\frac{\partial v_i}{\partial x_\alpha^+}+v_\alpha\frac{\partial\overline{V}_i}{\partial x_\alpha^+}=-\frac{\partial p}{\partial x_i^+}+\frac{\partial\sigma_{i\alpha}}{\partial x_\alpha^+}. \end{aligned}\right\} \tag{5.3}$$

Stress fluctuations σ_{ij} as well as fluctuations v_α, p (2.2) will be roughly approximated by the sinusoidal self-oscillations

$$\sigma_{ij}=\mathscr{R}[\sigma_{ij}(y^+)T],\quad T=2^{\frac{1}{2}}\exp\left[i(\alpha x^+ +\beta z^+)-i\alpha ct^+\right]. \tag{5.4}$$

After substitution of (2.2) and (5.4) into (5.3), a system of ordinary differential equations for the complex stress amplitudes can be obtained

$$\left.\begin{aligned} \sigma_{11}\chi &= 2i\alpha u+2A(U'u'+U'\sigma_{12}+2i\alpha AU'^2u-2AU'U''v),\\ \sigma_{12}\chi &= u'+i\alpha v+A(i\alpha U'u+U'\sigma_{22}+U'v'-U''v'+2i\alpha AU'^2v),\\ \sigma_{22}\chi &= 2v'+2i\alpha AU'v,\\ \sigma_{23}\chi &= i\beta v+w'+i\alpha AU'w,\\ \sigma_{13}\chi &= i\beta u+i\alpha w+A(U'\sigma_{23}+U'w'+2i\alpha U'^2w),\\ \sigma_{33}\chi &= 2i\beta w, \end{aligned}\right\} \tag{5.5}$$

where $\chi=1+i\alpha A(U-c)$. After solving (5.5) with respect to σ_{ij} and then substituting the obtained expressions into the equation of motion, we obtain

$$\left.\begin{aligned} &i\alpha\chi(U-c)u+\chi U'v+i\alpha\chi p\\ &\quad=u''+2\chi'u'+(\chi''+2\chi'^2-k^2)u+\frac{\chi'}{i\alpha\chi}[v''+2\chi'v'+(\chi''+2\chi'^2-k^2)v]\\ &\qquad+\frac{2\chi''}{i\alpha\chi}v'-\frac{1}{i\alpha}\left(\chi'''-\frac{2\chi'\chi''}{\chi}\right)v,\\ &\qquad i\alpha\chi(U-c)v+\chi p'=v''+2\chi'v'+(\chi''+2\chi'^2-k^2)v,\\ &\qquad i\alpha\chi(U-c)w+i\beta\chi p=w''+2\chi'w'+(\chi''+2\chi'^2-k^2)w,\\ &\qquad v'+i\alpha u+i\beta w=0. \end{aligned}\right\} \tag{5.6}$$

Assuming that $U^+=y^+$ and eliminating p in (5.6), we obtain the following system of ordinary differential equations for the fluctuation amplitudes

$$\left.\begin{aligned} \phi''-\frac{2\chi'}{\chi}\phi'+\left(\frac{2\chi'^2}{\chi^2}-k^2\right)\phi-i\alpha\chi(y^+-c)(v''-k^2v)=0.\\ v''+2\chi'v'+(2\chi'^2-k^2)v-\phi=0,\\ w''+2\chi'w'+[2\chi'^2-k^2-i\alpha\chi(y^+-c)]w=\frac{i\beta}{k^2}\left\{\phi'-\frac{\chi'}{\chi}\phi-i\alpha\chi[(y^+-c)v'-v]\right\},\\ u=\frac{i}{\alpha}(v'+i\beta w),\\ p=\frac{1}{k^2\chi}\left\{\phi'-\frac{\chi'}{\chi}\phi-i\alpha\chi[(y^+-c)v'-v]\right\}. \end{aligned}\right\} \tag{5.7}$$

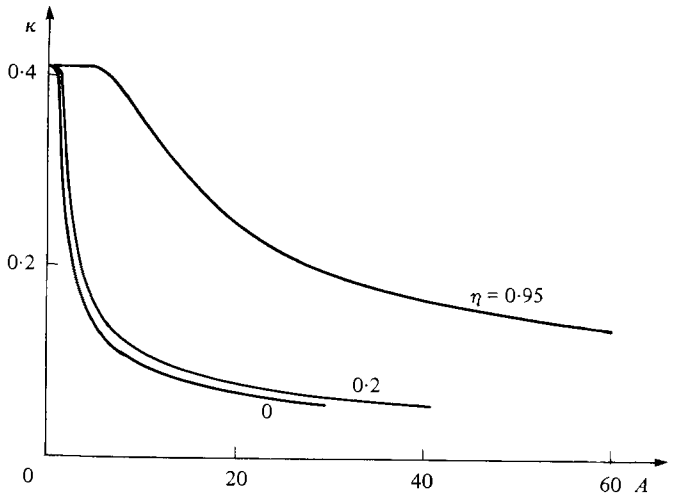

FIGURE 3. Factor κ of the logarithmic mean-velocity profile in 'buffer' region.

Hence the fluctuational motion near the wall is determined by integrating (5.7), whose boundary conditions imply no slip on the wall (2.7) and the absence of the effect of viscosity and elasticity far from the wall (2.8). The conditions of intermediate normalization, i.e.

$$v = a \quad \text{at} \quad y^+ = R, \tag{5.8}$$

presets the amplitude factor module, and closes the problem (5.7), (2.7), (2.8) and (5.8). The generalized Reynolds equations (5.2) after substituting the known solution permit us to determine a nonlinear profile of the mean velocity.

According to the above, the mean velocity and energy in the 'buffer' region can, for reasons of dimensionality, be expressed through (2.3) and (2.4). Hence, for the determination of sinusoidal fluctuation parameters the previous conditions of closing are retained. Let the mean velocity gradient be expressed as $U' = (1+\varphi)/(1+\psi)$, where φ and ψ are the linear functions with respect to the second-order moments specified by (5.2). The values of φ and ψ are calculated through the intermediate normalization (5.8), and the scale factor D is determined from the first condition of (2.10) which, taking into account the introduced designations, will take the form

$$D^4 + [R(\varphi' - \psi') + \varphi + \psi]\, D^2 + R(\varphi'\psi - \varphi\psi') + \varphi\psi = 0. \tag{5.9}$$

After the determination of D, the mean velocity profile is found by integrating the generalized Reynolds equations (5.2) in the range $0 \leqslant y \leqslant R$, beyond which it is continued logarithmically with coefficients calculated from (2.15). Hence the mean-velocity profile is determined over the whole region of the effect of fluid viscosity and elasticity except for its external boundary.

The algorithm of the solution of the problem is similar to that for a Newtonian fluid. The only difference is that the first two equations of (5.7) are coupled. Therefore they are integrated by the method of finite-difference factorization with the boundary conditions $v = v' = 0$ on the wall and $v = a$, $v'' - k^2 v = 0$ at $y^+ = R$. Among the four roots of the biquadratic equation (5.9), the real positive is chosen. In the overall range of the elasticity criterion A under study this root did exist and was the only one.

A numerical solution of the problem was performed via the continuous transition

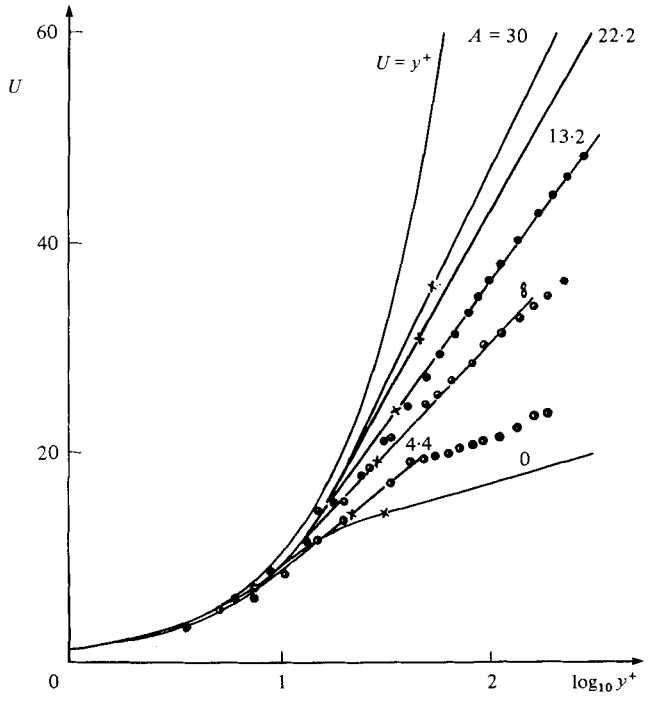

FIGURE 4. Comparison of calculated mean-velocity profiles of viscoelastic Maxwell fluid with experimental data by Khabakhpasheva & Perepelitza (1970); ×, conjunction points.

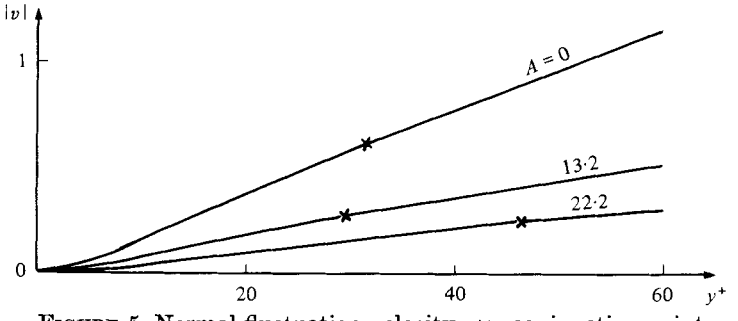

FIGURE 5. Normal fluctuation velocity: ×, conjunction points.

with respect to the parameter A. For a special case $A = 0$ (Newtonian fluid) values of all parameters of the solution coincide with the above ((2.14) and (2.16)). With increasing A from 0 to A_* which will be referred to as the threshold value ($A_* \simeq 1$), the solution is practically independent of A. Figure 3 illustrates variations of the coefficient κ of the mean-velocity logarithmic region as a function of A ($\eta = 0$). Deviation from the Newtonian flow starts at $A > A_*$, κ being reduced. The existence of a threshold temporal-type value agrees with the experiments of Berman (1977).

The calculated mean-velocity profiles are in good quantitative agreement with experiment (figure 4). Measurement results were taken from the work of Khabakhpasheva & Perepelitza (1970). At an insignificant drag reduction when the length of the 'buffer' region is small ($A = 4{\cdot}4$), experimental points also lie on the second logarithmic region of the mean-velocity profile.

As seen from figure 4, in a flow of the Maxwell fluid the thickness of the viscous

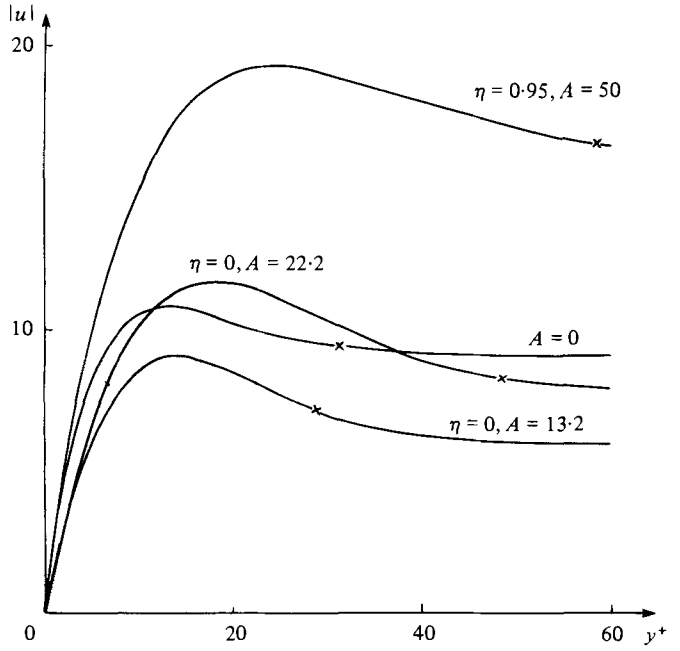

FIGURE 6. Longitudinal fluctuation velocity: ×, conjunction points.

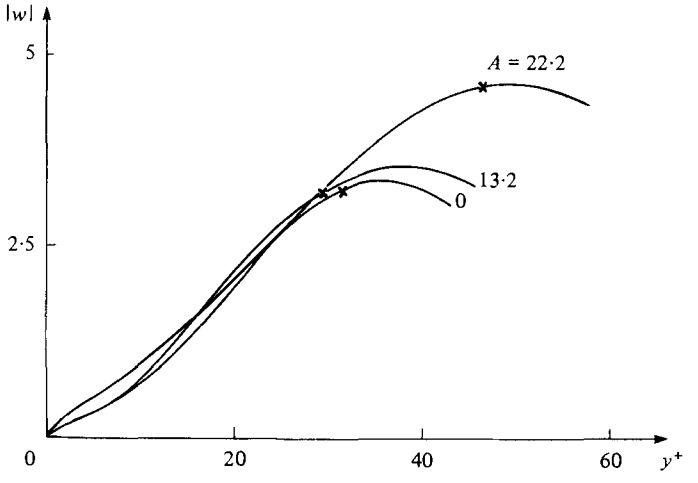

FIGURE 7. Transverse fluctuation velocity: ×, conjunction points.

sublayer does not increase. Profiles of the mean velocity in the near-wall region ($y^+ < 10$) are localized at a small distance from the linear profile, but deviate from it already at $y^+ = 3$–5. The available experimental data by Khabakhpasheva & Perepelitza (1970) correspond to the obtained results.

The intensity distribution of turbulent fluctuations qualitatively agrees with experiment. The normal fluctuation velocity decreases in the range under study by a factor of 2–3 times the increase in A (figure 5). Longitudinal and transverse components change insignificantly (figures 6 and 7), though it can be noted that near the wall they slightly decrease.

Hence, on the basis of elementary theory formulated here for a viscous sublayer in terms of the Maxwell viscoelastic fluid without application of any empirical constants, the main features characterizing the drag reduction in dilute polymer solutions can be obtained. Therefore it can be concluded that the viscoelastic properties of solutions play a decisive role in drag reduction. The agreement between theory and experiment is attained at A values of the order of magnitude corresponding to measurements for dilute polymer solutions. Thus $A = 4{\cdot}4$ (figure 4) corresponds to $\lambda = 1{\cdot}3 \times 10^{-3}$ s, and according to the Hoyt's (1972) experimental data $\lambda \sim 10^{-3}$ s.

6. Viscous layer in Oldroyd fluid

A Maxwell model that provides a theoretical interpretation for the drag-reduction effect, possesses, nevertheless, a definite internal shortcoming. In this model the stress jump leads to infinite deformation velocities, which is in disagreement with the observed properties of polymer solutions. In addition, in what follows it will be shown that not all observed properties of the studied solutions can be described in this way. Therefore, for a more detailed analysis of the drag reduction in viscoelastic fluids, we will generalize the model viscous-layer theory for a more realistic Oldroyd fluid having stress relaxation and retardation times. The constitutive equation for the Oldroyd (1950) medium is

$$\Sigma_{ij} + \lambda\left(\frac{\partial \Sigma_{ij}}{\partial t} + V_\alpha \frac{\partial \Sigma_{ij}}{\partial x_\alpha} - \frac{\partial V_i}{\partial x_\alpha}\Sigma_{\alpha j} - \frac{\partial V_j}{\partial x_\alpha}\Sigma_{i\alpha}\right) = 2\nu\left[\dot{e}_{ij} + \eta\lambda\left(\frac{\partial \dot{e}_{ij}}{\partial t} + V_\alpha \frac{\partial \dot{e}_{ij}}{\partial x_\alpha} - \frac{\partial V_i}{\partial x_\alpha}\dot{e}_{\alpha j} - \frac{\partial V_j}{\partial x_\alpha}\dot{e}_{i\alpha}\right)\right], \tag{6.1}$$

where

$$\dot{e}_{ij} = \frac{1}{2}\left(\frac{\partial V_i}{\partial x_j} + \frac{\partial V_j}{\partial x_i}\right)$$

is the tensor of strain velocities, λ is the time of stress relaxation, $\eta\lambda$ is the retardation time and $0 \leqslant \eta < 1$. The rheological Maxwell equation (5.1) is a special case of (6.1) corresponding to $\eta = 0$.

Equations of the averaged motion, being generalized Reynolds equations, have the dimensionless form

$$\left.\begin{aligned} \frac{dU}{dy^+}(1 + A\bar{\sigma}_{22}) &= 1 + \overline{v_x v_y} + A\left[\overline{v_y\left(\frac{\partial \sigma_{11}}{\partial x^+} + \frac{\partial \sigma_{12}}{\partial y^+} + \frac{\partial \sigma_{13}}{\partial z^+}\right)}\right. \\ &\quad \left. + \overline{v_x\left(\frac{\partial \sigma_{21}}{\partial x^+} + \frac{\partial \sigma_{22}}{\partial y^+} + \frac{\partial \sigma_{23}}{\partial z^+}\right)} - \frac{\partial \overline{\sigma_{22} v_x}}{\partial y^+}\right] \\ &\quad - \eta A\left[\overline{v_y \Delta v_x} + \overline{v_x \Delta v_y} - 2\frac{\partial}{\partial y^+}\left(\overline{v_x \frac{\partial v_y}{\partial y^+}}\right)\right], \\ \bar{\sigma}_{22} &= A\left[\frac{\partial \overline{\sigma_{22} v_y}}{\partial y^+} - 2\overline{v_y\left(\frac{\partial \sigma_{21}}{\partial x^+} + \frac{\partial \sigma_{22}}{\partial y^+} + \frac{\partial \sigma_{23}}{\partial z^+}\right)}\right] \\ &\quad + 2\eta A\left[\overline{v_y \Delta v_y} - \frac{\partial}{\partial y^+}\left(\overline{v_y \frac{\partial v_y}{\partial y^+}}\right)\right]. \end{aligned}\right\} \tag{6.2}$$

In the system of equations for the fluctuational motion let us remove the terms that

are quadratic with respect to fluctuations, and then carry out several successive rather cumbersome but practically simple transformations similar to the above operations and finally we will come to a system of ordinary differential equations for the sinusoidal fluctuation amplitudes, being the generalization of (5.7):

$$\left.\begin{aligned}
&\phi''-\frac{2\chi'}{\chi}\phi'+\left(\frac{2\chi'^2}{\chi^2}-k^2\right)\phi-i\alpha\chi(y^+-c)\,(v''-k^2v)=0,\\
&\gamma(v''-k^2v)+2(\chi'-\gamma')v'+2\chi'(\chi'-\gamma')v-\phi=0,\\
&\gamma(w''-k^2w)+2(\chi'-\gamma')w'+[2\chi'(\chi'-\gamma')-i\alpha\chi(y^+-c)]w\\
&\quad=\frac{i\beta}{k^2}\left\{\phi'-\frac{\chi'}{\chi}\phi-i\alpha\chi[(y^+-c)v'-v]\right\},\\
&u=\frac{i}{\alpha}(v'+i\beta w),\\
&p=\frac{1}{k^2\chi}\left\{\phi'-\frac{\chi'}{\chi}\phi-i\alpha\chi[y^+-c)v'-v]\right\}.
\end{aligned}\right\} \tag{6.3}$$

Here $\gamma = 1+i\alpha\eta A(y^+-c)$. Boundary conditions for (6.3) remain as before.

A dimensional analysis is carried out in a similar manner to that in §5. If at a constant value of η we assume that $\lambda\to\infty$, we will find the range of distances from the wall where the intermediate asymptotic equations (2.3) and (2.4) are valid. Consequently, the conditions of smooth conjunction will have the same form as (2.10) and (2.12). The normalization condition (5.9) will also remain unchanged; only the expressions for the functions φ and ψ will be different.

The problem was solved numerically via the continuous transition regarding the parameter A at a constant η. The coefficient κ of the first logarithmic region of the mean velocity as a function of A for various η is illustrated in figure 3. As seen, the threshold value A_*, being equal to unity for Maxwell fluid, rises to 5–6 at $\eta\sim 0{\cdot}9$ with the increase of η.

As in a Maxwell fluid, the drag-reduction effect is observed with increasing A (figure 8). But depending on the parameter η the character of the velocity-profile behaviour changes. At large retardation times $\eta\sim 0{\cdot}9$, and at A values for the case of sufficiently high drag reduction, a distinct increase in the viscous-sublayer thickness is observed (figures 8 and 9), $\eta = 0{\cdot}95$. In this case the theoretical profiles are in good agreement with Rudd's (1972) experimental data. It should be noted that the calculated longitudinal fluctuating velocity, which is also in agreement with the Rudd's experiments, increases rather significantly (figure 6), $\eta = 0{\cdot}95$. The normal fluctuating component is damped.

The thickness of the viscous sublayer does not increase compared with the Newtonian flow at low retardation times (figure 9), $\eta = 0{\cdot}2$. In this case the flow structure in the near-wall layer is consistent with the above features characterizing the near-wall turbulence of the Maxwell viscoelastic fluid. To compare the calculated velocity profiles at $\eta = 0{\cdot}2$ with experiment, in figure 9 the experimental data of Khabakhpasheva & Perepelitza (1970) are given. The mean-velocity profiles deviate from linearity at $y^+ = 3$–5. Nevertheless, at small η, the extent of drag reduction is higher than in the case of large retardation times (figure 3). With increasing A, the drop of the coefficient κ is sharper and the slope of velocity profiles steepens faster.

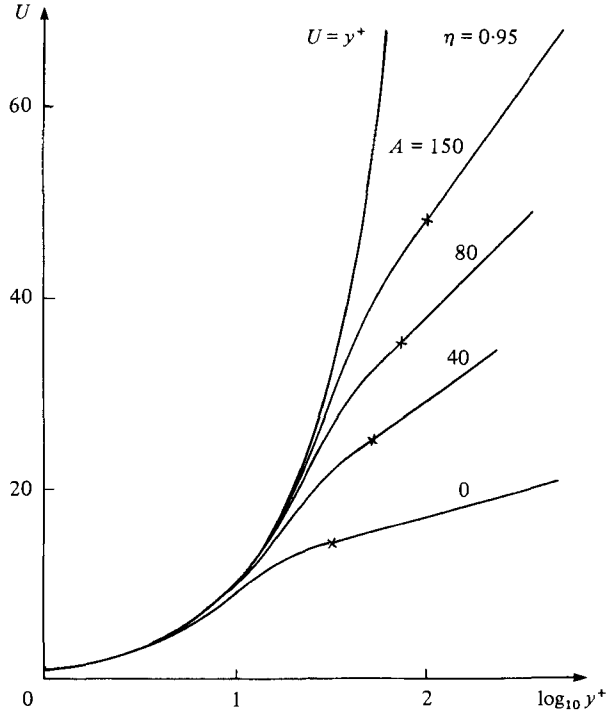

FIGURE 8. Calculated mean-velocity profiles of Oldroyd fluid: ×, conjunction points.

7. Discussion

The analysis of the near-wall turbulent flow of non-Newtonian Maxwell and Oldroyd media in terms of the developed theoretical approach indicates that the fluid elastic properties can change the structure of the viscous sublayer and buffer region significantly, and can account for the most essential effects observed experimentally in dilute polymer solutions. It holds primarily for the main effect of turbulent friction reduction and the associated decrease of the normal velocity fluctuations. The theory also describes the threshold character of the effect, implying that after the criterion A exceeds some value A_* the drag crisis takes place, i.e. it decreases sharply and significantly. The rheological property of retardation described by the parameter η smooths the critical character of the drag reduction and increases the threshold value A_*. It is likely that just this fact accounts for a slight scatter in the empirical temporal-type correlations determined at the point of onset of the drag reduction. A mechanism for the effect of elastic properties on a fluid flow will be evident if we analyse the stress state near the wall. Upon retaining the principal terms in the stress tensor that do not tend to zero on approaching to the wall, and subtracting the pressure, we obtain

$$\|\bar{\sigma}_{ij}\| = \begin{pmatrix} 2A(1-\eta)\left(U'^2 + \dfrac{\partial \bar{v}_x^2}{\partial y^+}\right) & U' & 0 \\ U' & 0 & 0 \\ 0 & 0 & 2A(1-\eta)\dfrac{\partial \bar{v}_z^2}{\partial y^+} \end{pmatrix}.$$

Hence the flow of viscoelastic fluid causes near the wall both shear and normal stresses

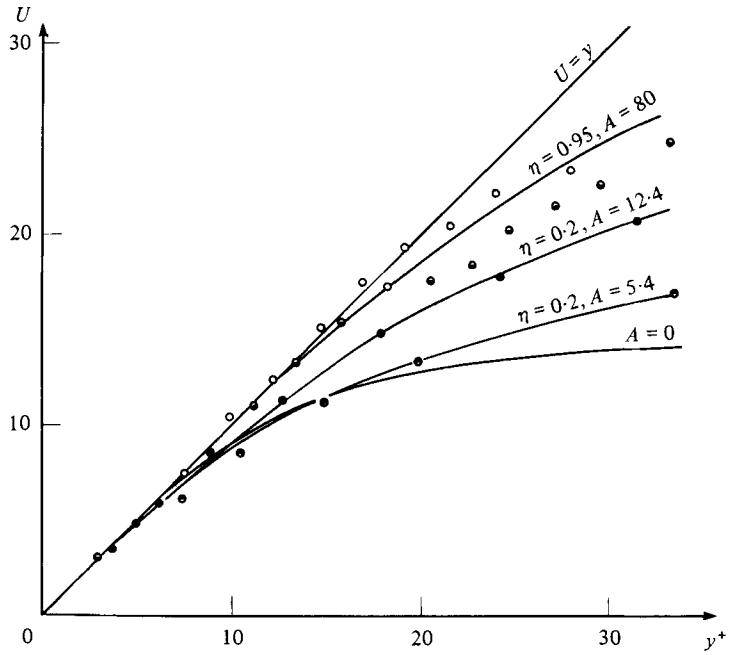

FIGURE 9. Calculated mean-velocity profiles of Oldroyd fluid in viscous sublayer: ○, ◒, experimental data of Rudd (1972); ●, ◓, experimental data of Khabakhpasheva & Perepelitza (1970).

$\overline{\sigma}_{11}$ and $\overline{\sigma}_{22}$. The effect, which is not small, is associated with the mean-velocity gradient U'. Besides the ordinary viscous friction, due to elastic properties, stretching stresses appear along the averaged streamlines, increasing with approach to the wall. The value $2A(1-\eta)$ is the ratio of the stretching to the viscous stresses (in near-wall scales $U'(0) = 1$). Experimental data for the relaxation times in polymer solutions provide values of $A \geqslant 4$, i.e. a significant value of the stretching stress. This fact can serve for the determination of rheological properties of the solutions under study.

The analysis of the stress tensor also clarifies a smoothing role of the retardation time, in particular the five- to sixfold and greater increase in the threshold values. If we expand the velocity profile in a Taylor series in the vicinity of $y^+ = 0$ and assume that $v_x = f(x^+, z^+, t^+)y^+ + \ldots$, $v_y = g(x^+, z^+, t^+)y^{+2} + \ldots$, we obtain

$$U' = 1 - 6A(1-\eta)\overline{fg}y^+ + \ldots + \overline{fg}y^{+3} + \ldots.$$

In contrast to the Newtonian case, when the unity is immediately followed by a cubic term, the elasticity of the medium leads to the appearance of linear terms in the expansion. If the thickness of the viscous sublayer is determined by the condition $|U'-1| < \epsilon$, at moderate values of $A(1-\eta)$ the stress relaxation decreases the sublayer thickness, whereas the retardation increases it. At large values of $A(1-\eta)$ we should take into account that f and g themselves depend on A and η.

These qualitative tendencies agree perfectly with numerical results regarding both the dependence of the threshold value of A_* on η (figure 3) and the viscous-sublayer thickness (figures 4 and 8). It is also clear that the stretching stresses, acting in the planes parallel to the wall and making them to be akin to elastic membranes, should damp the normal fluctuations v_y, but do not prevent the planes' mutual sliding. In

complete agreement with this, the calculation provides a decrease in the sublayer v_y (figure 5), whereas the components v_x and v_z retain their order of magnitude (figures 6 and 7).

In conclusion it should be noted that the developed non-empirical theory of near-wall turbulence permits us to perform a correct calculation of the mean-velocity distribution and several fluctuational-motion characteristics for a whole class of problems associated with turbulent flows of fluids with different rheological properties.

It has been shown that in a turbulent flow of the Maxwell and Oldroyd media the phenomena typical of the Toms effect are observed. In a certain sense a viscoelastic fluid is even more convenient for the application of the above theoretical model, since in this case fluctuations become larger scale, thus giving more grounds for the linearization, and the spectrum narrows significantly, and hence the sinusoidal approximation becomes more accurate. The results permit us to hope that the theory can also be applied successfully to other near-wall flows having a rather simple structure of fluctuations in a viscous sublayer.

The authors wish to thank Professor S. S. Kutateladze for his constant support and valuable assistance making possible the performance of the present study.

REFERENCES

BERMAN, N. S. 1977 Flow time scales and drag reduction. *Phys. Fluids* **20**, 168–175.

CORCOS, G. M. 1964 The structure of the turbulent pressure field in boundary layer flow. *J. Fluid Mech.* **18**, 353–378.

CORINO, E. K. & BRODKEY, R. S. 1969 A visual investigation of the wall region in turbulent flows. *J. Fluid Mech.* **37**, 1–30.

DAVIES, P. O. A. & YULE, A. J. 1975 Coherent structures in turbulence. *J. Fluid Mech.* **69**, 513–537.

EINSTEIN, N. A. & LI, H. 1956 The viscous sublayer along a smooth boundary. *J. Engng Mech. Div. A.S.C.E.* **82**, 1–27.

GESHEV, P. I. 1974 Turbulent exchange coefficients in viscous sub-layers. *Prikl. Mekh. Teor. Fiz.* **2**, 61–66.

GOLDSHTIK, M. A. 1968 Criterion of maximum stability of averaged turbulent flows. *Dokl. Akad. Nauk S.S.S.R.* **182**, 1026–1028.

GOLDSHTIK, M. A. & SHTERN, V. N. 1977 *Hydrodynamic Stability and Turbulence.* Nauka.

GORODTZOV, V. A. & BELOKON, V. S. 1973 Similarity laws for developed turbulence in diluted polymer solutions. *J. Engng Phys.* **25**, 967–976.

HATZIAVRAMIDIS, D. T. & HANRATTY, T. J. 1979 The representation of the viscous wall region by a regular eddy pattern. *J. Fluid Mech.* **95**, 655–679.

HOYT, J. W. 1972 The effect of additives on fluid friction. *Trans. A.S.M.E.* D, *J. Basic Engng* **94**, 258–285.

KADER, B. A. 1970 Turbulence in viscous sub-layer near a flat wall. In *Turbulent Flows*, pp. 69–73. Nauka.

KHABAKHPASHEVA, E. M., MIKHAILOVA, E. S., PEREPELITZA, B. V. & EFIMENKO, G. I. 1975 Experimental studies of the structure of near-wall turbulence. In *Near-Wall Turbulent Flows*, part 2, pp. 138–161. Institute of Thermophysics, Novosibirsk.

KHABAKHPASHEVA, E. M. & PEREPELITZA, B. V. 1970 Peculiarities of near-wall turbulence in water flows with high-molecular additives. *J. Engng Phys.* **18**, 1094–1097.

KLINE, S. J., REYNOLDS, W. S., SHRAUB, F. A. & RUNSTADLER, P. W. 1967 The structure of turbulent boundary layers. *J. Fluid Mech.* **26**, 199–221.

LAUFER, J. 1954 The structure of turbulence in fully developed pipe flow. *NACA Rep.* no. 1174.

LAWN, C. J. 1971 The determination of the rate of dissipation in turbulent pipe flow. *J. Fluid Mech.* **48**, 477–508.

METZNER, A. B. & PARK, M. G. 1964 Turbulent flow characteristics of viscoelastic fluids. *J. Fluid Mech.* **20**, 291–303.

MITCHELL, J. E. & HANRATTY, T. J. 1966 A study of turbulence at a wall using an electrochemical wall shear-stress meter. *J. Fluid Mech.* **26**, 199–221.

MORRISON, W. R. B., BULLOCK, K. J. & KRONAUER, R. E. 1971 Experimental evidence of waves in the sublayer. *J. Fluid Mech.* **47**, 639–656.

OLDROYD, J. G. 1950 On the formulation of rheological equations of state. *Proc. R. Soc. Lond.* A **200**, 523–541.

REPIK, E. U., SOSEDKO, YU. P. & TROPININA, N. S. 1975 Studies of flow structure in the near-wall region of turbulent boundary layers. In *Near-Wall Turbulent Flows*, part II, pp. 138–161. Institute of Thermophysics, Novosibirsk.

RUDD, M. J. 1972 Velocity measurements made with a laser dopplermeter on the turbulent pipe flow of dilute polymer solutions. *J. Fluid Mech.* **51**, 673–685.

SADOVSKII, V. S., SINITZYNA, I. P. & TAGANOV, G. I. 1975 Numerical studies of a mathematical model for a viscous flow in turbulent boundary layer. In *Near-Wall Turbulent Flow*, part 1, pp. 94–116. Institute of Thermophysics, Novosibirsk.

SCHUBERT, G. & CORCOS, G. M. 1967 The dynamics of turbulence near a wall according to a linear model. *J. Fluid Mech.* **29**, 113–135.

STERNBERG, J. 1962 A theory for the viscous sublayer of a turbulent flow. *J. Fluid Mech.* **13**, 241–271.

TOMS, B. A. 1949 Some observations on the flow of linear polymer solutions through straight tubes at large Reynolds number. In *Proc. 1st Int. Cong. Rheol.*, vol. II, pp. 135–144. Amsterdam.

TOWNSEND, A. A. 1956 *The Structure of Turbulent Shear Flow*. Cambridge University Press.